J|A|C|S
ARTICLES
Published on Web 01/23/2004

# Noncovalent Interactions: Defining Cooperativity. Ligand Binding Aided by Reduced Dynamic Behavior of Receptors. Binding of Bacterial Cell Wall Analogues to Ristocetin A

Dudley H. Williams,* Nichola L. Davies, Rosa Zerella, and Ben Bardsley

*Contribution from the Department of Chemistry, University of Cambridge, Lensfield Road, Cambridge CB2 1EW, U.K.*

Received November 4, 2003; E-mail: dhw1@cam.ac.uk

***Abstract:*** Changes in the relative populations of the monomer and asymmetric dimer forms of ristocetin A, upon binding of two molecules of ligand, suggest that ligand binding is negatively cooperative with respect to dimerization. However, strong hydrogen bonds formed in the binding sites of the ligands are reinforced in the dimer relative to the monomer, and the barrier to dissociation of the dimer is increased upon binding of the ligands. It is concluded that the interactions which are common in the binding of both ligands are made with positive cooperativity with respect to those involved in dimerization. The conclusions are relevant to the binding of ligands to proteins, where ligand binding energy can be derived from stabilization of the protein in its ligand-bound form.

## Introduction

Cooperative interactions between sets of noncovalent bonds are crucial in biology. They allow the free energy change associated with binding events to be modulated, and the geometry of receptors to be changed upon ligand binding.[1−4] This latter property allows signal transduction.[5] The papers of Monod, Wyman, and Changeux (MWC) on positively cooperative binding,[6] and of Koshland and colleagues on negatively cooperative binding,[5,7] consider cases where there are multiple ligand binding sites in the receptor. Binding is defined to be positively cooperative where the binding curve for ligand binding is sigmoid in shape (i.e., the first-bound ligand is bound more weakly to the receptor than are subsequently bound ligands). Binding is defined to be negatively cooperative where the first-bound ligand is bound more strongly to the receptor than are subsequently bound ligands.

Here, we adopt different definitions of cooperativity. We take the view that sets of noncovalent interactions that are made with *positive* cooperativity must be mutually *enhancing* in their free energy benefits. Conversely, sets of noncovalent interactions that are made with *negative* cooperativity must be mutually *weakening* in their free energy benefits. This seemingly obvious requirement is often not met in binding events that are described as either positively or negatively cooperative. Indeed, binding that is described in the literature as positively cooperative (e.g., the binding of $O_2$ to hemoglobin)[6] is negatively cooperative using the definitions adopted here.[11]

**(i) Presently Used Definitions of Positively and Negatively Cooperative Binding.** The most common use of the term "positively cooperative" is where two, or more, sets of noncovalent interactions when expressed simultaneously give rise to a binding free energy that is more negative than the sum of the parts. Such positive cooperativity is typically found in the folding of proteins. Thus, fragments of proteins often fail to fold into the structures that they form when present in the whole protein and, even when they do, are commonly less stable than when present in the whole protein.[8,9] Conversely, where the interaction between two sets of noncovalent interactions gives rise to a binding energy that is less than the sum of the parts, the interaction between the two sets can be said to be negatively cooperative. We have used these definitions of positively and negatively cooperative binding, and illustrate here, and elsewhere,[10,11] that they have unifying structural consequences. These are (i) in the case of positive cooperativity, decreased dynamic behavior of a receptor system (with a benefit in enthalpy and a cost in entropy) and (ii) in the case of negative cooperativity, increased dynamic behavior of a receptor system (with a cost in enthalpy and a benefit in entropy).

A model for such cooperative binding is given in Figure 1. Ligand binding can modify the distances and angles of the noncovalent interactions within the receptor, but does not break them, nor lead to the formation of new interactions. The pro-

(1) Benkoussa, M.; Nomine, B.; Mouchon, A.; Lefebvre, B.; Bernardon, J. M.; Formstecher, P.; Lefebvre, P. *Recept. Signal Transduction* **1997**, *7*, 257−267.
(2) Freire, E. *Proc. Natl. Acad. Sci. U.S.A.* **1999**, *96*, 10118−10122.
(3) Roux, S.; Terouanne, B.; Couette, B.; Rafestin-Oblin, M. E.; Nicolas, J. C. *J. Biol. Chem.* **1999**, *274*, 10059−10065.
(4) Shoelson, S. E.; Sivaraja, M.; Williams, K. P.; Hu, P.; Schlessinger, J.; Weiss, M. A. *EMBO J.* **1993**, *12*, 795−802.
(5) Biemann, H.-P.; Koshland, D. E. *Biochemistry* **1994**, *33*, 629−634.
(6) Monod, J.; Wyman, J.; Changeux, J.-P. *J. Mol. Biol.* **1965**, *12*, 88−118.
(7) Koshland, D. E.; Nemethy, G.; Filmer, D. *Biochemistry* **1966**, *5*, 365−385.
(8) Blanco, F. J.; Rivas, G.; Serrano, L. *Nat. Struct. Biol.* **1994**, *1*, 584−590.
(9) Wright, P. E.; Dyson, H. J.; Lerner, R. A. *Biochemistry* **1988**, *27*, 7167−7175.
(10) Williams, D. H.; Calderone, C. T.; O'Brien, D. P.; Zerella, R. *Chem. Commun.* **2002**, *12*, 1266−1267.
(11) Williams, D. H.; Stephens, E.; Zhou, M. *J. Mol. Biol.* **2003**, *329*, 389−399.


**10.1021/ja039409p CCC: $27.50** 

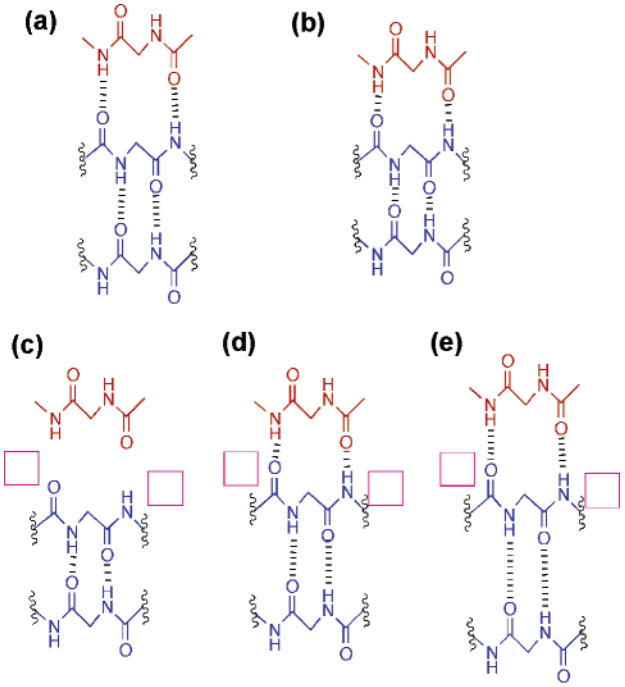


***Figure 1.*** Schematic representation of a ligand (red) binding to a receptor (blue). The receptor may be a single entity, or may consist of noncovalently connected species (e.g., a dimer). (a) Ligand binding in the absence of cooperativity. (b) Ligand binding with positive cooperativity. (c−e) Ligand binding with negative cooperativity. (c) Steric inhibition (maroon squares) toward ligand binding. (d) The steric inhibition toward ligand binding causes distortion of the otherwise preferred receptor structure, with a reduction in efficiency of bonding in its internal hydrogen bond network. (e) Further loosening of the receptor structure since the reduction in bonding in step d allows an increase in dynamic behavior of the receptor, which in turn further decreases its internal bonding efficiency (enthalpy/entropy compensation). Where the tightened (b) or loosened (d, e) interactions are coupled to other interactions within the receptor system, they will be similarly affected.

posed structural consequences of positively cooperative binding are represented by the transformation (a) → (b) in Figure 1. They may occur where the ligand can form its noncovalent bonding pattern to the receptor without significant distortion of the structure of the receptor. In Figure 1a, the ligand (red) forms hydrogen bonds to the receptor (blue) without the benefit of positive cooperativity. That is, the ligand−receptor hydrogen bonds are formed without permitting the receptor to modify its internal hydrogen-bonding structure. However, in reality, the binding of the ligand reduces the dynamic behavior of the surface peptide backbone to which it binds. This reduction in dynamic behavior of the surface peptide backbone in turn allows an increase in the strength of the hydrogen-bonding network within all parts of the receptor that are coupled to ligand binding with positive cooperativity. The structural consequence of positively cooperative binding is shortening of the noncovalent bonds that are involved [(a) → (b) in Figure 1, with distance changes exaggerated for the purpose of illustration].[12] There is thereby a widespread reduction in the dynamic behavior of the interfaces. This has been established by reduced amide backbone H/D exchange within the streptavidin receptor upon binding biotin.[11] Since the positive cooperativity occurs with an improvement in bonding and a reduction in dynamic behavior, it also occurs with a benefit in enthalpy and a cost in entropy.[10,13,14]

In negatively cooperative binding, making simultaneously the two sets of bonds in the preferred geometry that would occur if each set were made alone is not possible. A model to illustrate the structural consequences of negatively cooperative binding is given by the changes (c) → (d) → (e) in Figure 1. The physical model for an increase in receptor dynamics upon the exercise of negative cooperativity involves arguing via two hypothetically separated steps. The first step is that the ligand binds by making noncovalent bonds to the receptor whose formation demands distortion of the noncovalent bonds that previously existed within the receptor. For example, there may be steric hindrance (see maroon squares in Figure 1c) that opposes the making of ligand−receptor hydrogen bonds to the initially available form of the receptor. Thus, the making of the ligand−receptor bonds involves extension of some of the hydrogen bonds within the receptor (Figure 1d), with a cost in enthalpy. In the second step, the dynamic consequences of this cost in enthalpy are considered. The decrease in bonding within the receptor will result in an increase in its dynamic behavior, which will in turn cause a further cost in enthalpy [see the further hydrogen bond extensions displayed in (d) → (e) in Figure 1]. Enthalpy/entropy compensation occurs to minimize the adverse change in free energy. We have given instances of the costs in enthalpy, and benefits in entropy, of negatively cooperative binding,[10] and have demonstrated the increase in dynamic behavior of hemoglobin upon binding of oxygen, which is *negatively* cooperative employing the definitions used here.[11]

**(ii) Ligand Binding to Ristocetin A. Positively or Negatively Cooperative?** In aqueous solution, the antibiotic ristocetin A (receptor) binds the bacterial cell wall analogue di-*N*-Ac-Lys-D-Ala-D-Ala (ligand) with a binding constant of $6 \times 10^5$ $M^{-1}$.[15] The antibiotic forms an asymmetric dimer ($D_1D_2$)[16] that is in equilibrium with monomer (M) ($K_{dim} = 300-800$ $M^{-1}$ under various near physiological conditions[16−18]). The above ligand binds to both the monomeric and dimeric forms of the antibiotic, but with somewhat different binding constants.[17,18] A structural representation of the ligand-bound asymmetric dimer is given in Figure 2, and a schematic representation is given in Figure 3a.

The asymmetry of the dimer arises because two tetrasaccharide units of ristocetin A are, in the dimer, packed together in a head-to-head manner, whereas the peptide backbones in the dimer are hydrogen bonded to each other in a head-to-tail manner (Figure 3a). As a consequence, when ligand binds to the dimer, it must do so in two different binding sites. The site of higher affinity is designated $D_1$, and that of lower affinity as $D_2$. There is evidence that the $D_1$ site is that in which the 6-methyl group of rhamnose lies in close proximity to the N-terminus of the ligand (Figure 3).[17,19] In this connection, we note that when a ligand binds to the M form of ristocetin A, it is clear that it binds to a site in which the tetrasaccharide has the same orientation as in a $D_1$ site.[20]

(12) Williams, D. H.; Maguire, A. J.; Tsuzuki, W.; Westwell, M. S. *Science* **1998**, *280*, 711−714.
(13) Calderone, C.; Williams, D. H. *J. Am. Chem. Soc.* **2001**, *123*, 6262−6267.
(14) Williams, D. H.; O'Brien, D. P.; Bardsley, B. *J. Am. Chem. Soc.* **2001**, *123*, 737−738.
(15) Nieto, M.; Perkins, H. R. *Biochem. J.* **1971**, *124*, 845−852.
(16) Waltho, J. P.; Williams, D. H. *J. Am. Chem. Soc.* **1989**, *111*, 2475−2480.
(17) Cho, Y.; Maguire, A.; Try, A. C.; Groves, P.; Westwell, M. S.; Williams, D. H. *Chem. Biol.* **1996**, *3*, 207−215.
(18) McPhail, D.; Cooper, A. *J. Chem. Soc., Faraday Trans.* **1997**, *93*, 2283−2289.
(19) Groves, P.; Searle, M. S.; Waltho, J. P.; Williams, D. H. *J. Am. Chem. Soc.* **1995**, *117*, 7958−7964.

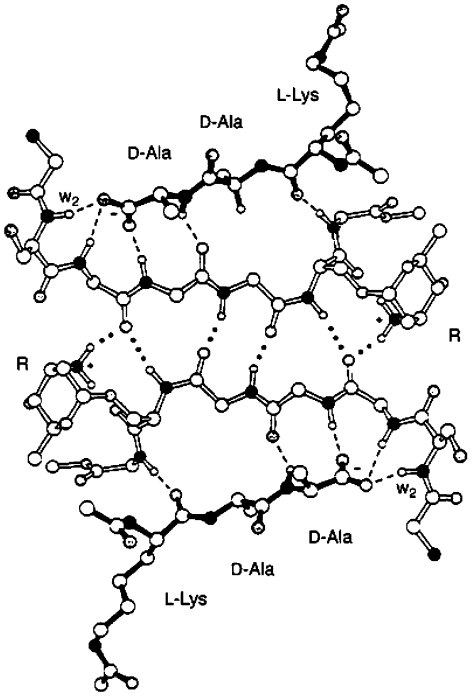


***Figure 2.*** Part of the structure of the ristocetin A ligand-bound complex. Reprinted from ref 19. Copyright 1995 American Chemical Society. The peptide backbone of the dimer is indicated by unfilled bonds, and bound di-*N*-Ac-L-Lys-D-Ala-D-Ala by filled-in bonds. Dimer interfacial hydrogen bonds are indicated by dotted lines, and ligand binding hydrogen bonds by broken lines. Key: carbon, open circles; nitrogen, black circles; oxygen, shaded circles. The amide NH $w_2$ (discussed in the text) is labeled.

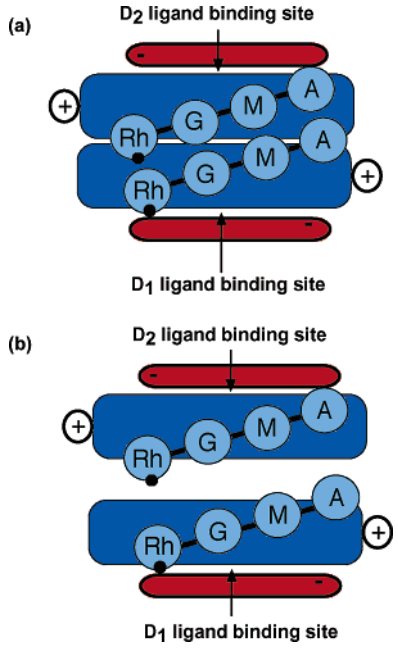


***Figure 3.*** (a) Schematic representation of the ristocetin A ligand-bound complex: ligands (red), peptide portions of ristocetin A (dark blue), and sugars (light blue). Rh = rhamnose, G = glucose (which gives the point of attachment to the peptide portion of the antibiotic), M = mannose, and A = arabinose. The 6-methyl group of rhamnose (used as a probe of the dimer ↔ monomer equilibrium) is indicated by a black circle. The negatively charged carboxylate termini of the ligands and the positively charged amino termini of the antibiotics are indicated by − and + signs, respectively. (b) Schematic illustration of the transition state for dissociation of the dimer. Since the tetrasaccharide has an extended structure (pivoting at the glucose residue), it is unable to rotate through 180° (as is necessary to convert a $D_2$ site to a $D_1$ site) as dimer dissociation proceeds. A cost of occupying a $D_2$ site therefore remains in the transition state for dissociation of the dimer.

The utility of this system is that the ristocetin A is a dimeric receptor system in which the monomer/dimer equilibrium is readily monitored by proton NMR spectroscopy both in the absence and in the presence of ligand. The rhamnose 6-methyl (location indicated in Figure 3) gives a resonance that occurs at very different chemical shifts according to whether it is positioned in a $D_1$ or a $D_2$ site of the dimer, or in the monomer. Additionally, the region in which these three resonances occur is free from other resonances (Figure 4a), allowing determination of the dimer/monomer ratio and hence of $K_{dim}$. When di-*N*-Ac-Lys-D-Ala-D-Ala is employed as the ligand, $K_{dim}$ rises from 830 ± 50 to 1250 ± 80 $M^{-1}$ after the addition of 0.5 equiv of the ligand (283 K, pH 7).[17] When the ligand is titrated into a solution of the antibiotic, it is clear that this 0.5 equiv of the ligand binds very largely to the $D_1$ site of the dimer, or to the site in the monomer. This follows since the affinity of binding to the $D_1$ site is, compared to that to the $D_2$ site, greater in the dimer by a factor of 7, but the $D_1$ site has an affinity for the ligand which is greater than that for the M site by a factor of only 1.6.[17] The increase in $K_{dim}$ upon ligand binding shows that the dimer with the $D_1$ site occupied is more stable (with respect to monomer with the $D_1$ site occupied) than is the free dimer (with respect to monomer) by 1 kJ $mol^{-1}$. Thus, in terms of the changes in population of the dimer, the binding of this ligand to the $D_1$ site is positively cooperative with respect to dimerization.

When a further 0.5 equiv of the ligand is added, $K_{dim}$ falls from 1250 ± 80 to 580 ± 50 $M^{-1}$ (283 K, pH 7). Thus, employing a definition of cooperativity that is based upon the changes in the population of the dimer, the binding of ligand to the $D_2$ site is negatively cooperative with respect to dimerization[17] by 1.8 kJ $mol^{-1}$. Moreover, the binding of ligands to both the $D_1$ and $D_2$ sites would appear to be negatively cooperative overall (580 ± 50 $M^{-1}$ < 830 ± 50 $M^{-1}$) by ca. 0.8 kJ $mol^{-1}$.

The structural proposals regarding positively and negatively cooperative binding (Figure 1) have been developed since the above data were acquired. One of the consequences of positively cooperative binding of a ligand to a receptor is an increase in the barriers to the dissociation of noncovalent interfaces within the receptor that are coupled with positive cooperativity to the ligand binding.[21] It is for this reason that the receptor system becomes less dynamic upon positively cooperative binding of ligand, and some of the amide backbone NH's of protein receptors then undergo less H/D exchange.[11] Conversely, we find that negatively cooperative binding of a ligand to a receptor system decreases the barriers to the disruption of noncovalent interfaces within the receptor that are coupled with negative cooperativity to the ligand binding.[11]

However, inspection of the published data[17] for the binding of 2 equiv of di-*N*-Ac-Lys-D-Ala-D-Ala to the ristocetin A dimer shows that in this case the effect of ligand binding is to *raise* the barrier to monomer/dimer exchange. Thus, in Figure 3 of the paper by Cho et al.,[17] the sharpening of the resonances due to the rhamnose 6-methyl group, of both dimer and monomer, upon binding of 2 equiv of ligand establishes that the barrier to

(20) Groves, P.; Searle, M. S.; Chicarelli-Robinson, I.; Williams, D. H. *J. Chem. Soc., Perkin Trans. 1* **1994**, 659−665.

(21) Shiozawa, H.; Chia, B. C. S.; Davies, N. L.; Zerella, R.; Williams, D. H. *J. Am. Chem. Soc.* **2001**, *124*, 3914−3919.

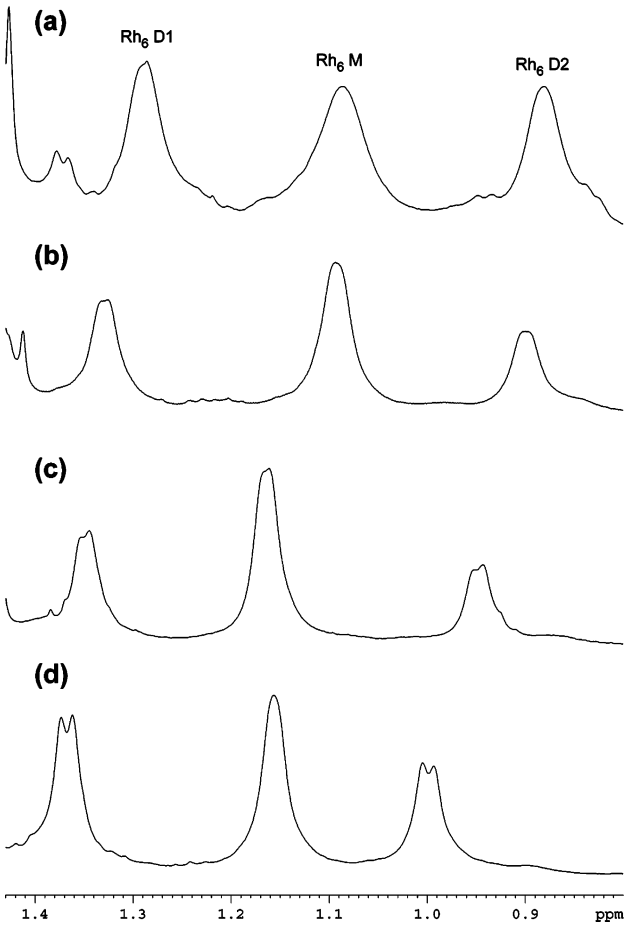


***Figure 4.*** Partial proton NMR spectra of ristocetin A (7 mM, 280 K, pH 4.5) showing the rhamnose 6-methyl chemical shifts in the $D_1$, $D_2$, and M sites (a) in free ristocetin A, and in ristocetin A (b) with bound Ac-Gly, (c) with bound Ac-Gly-Gly, and (d) with bound Ac-Gly-Gly-Gly.

monomer/dimer exchange is raised by ligand binding. We confirm this conclusion subsequently by a direct measurement of the barrier (see later).

In summary, the published work on risocetin A leads to an apparent inconsistency. In terms of population changes, the binding of two molecules of ligand is concluded to be negatively cooperative. Yet the barrier to monomer/dimer exchange increases upon ligand binding, suggesting positively cooperative binding of the ligand. In the present paper, we resolve this dilemma and show that there is no inconsistency.

## Results and Discussion

**(i) Generality of the Dilemma.** First, we wished to see if the dilemma was a more general one found in the binding of ligands to ristocetin A. Ac-Gly, Ac-Gly-Gly, and Ac-Gly-Gly-Gly were used as ligands, and the relevant data from these studies are presented in Figure 4b−d. The degree of complexation was in all cases ≥90% by use of an appropriate excess of ligand. Using *the criterion of relative population* of dimer vs monomer signals, $D_1 + D_2$ resonances would have to increase relative to M resonances upon the binding of the ligands to allow the conclusion that ligand binding is positively cooperative with respect to dimerization. This is not the case as can be seen by simple observation of the relative intensities (Figure 4), or by integration. The intensities of the $D_1 + D_2$ resonances are, relative to those of M, reduced. Therefore, including also the

***Table 1.*** Values of $K_{dim}$, $\Delta G_{dim}$, Barriers to Dimer Dissociation ($\Delta G^{\ddagger}$), and Ligand Binding Constants ($\Delta G_{lig}$) for Ristocetin A and Ristocetin A/Ligand Complexes[a]

| | $K_{dim}$ (±20 $M^{-1}$) | $\Delta G_{dim}$ (±0.5 kJ $mol^{-1}$) | $\Delta G^{\ddagger}$ [b] | $\Delta G_{lig}$ (±1 kJ $mol^{-1}$) |
|---|---|---|---|---|
| free ristocetin A | 350 | −13.6 | 60.5 | |
| ristocetin A/Ac-Gly | 200 | −12.3 | 61.5 | −11[c] |
| ristocetin A/Ac-Gly-Gly | 160 | −11.8 | 62.6 | −15.6[d] |
| ristocetin A/Ac-Gly-Gly-Gly | 320 | −13.5 | 63.6 | −16.2[e] |
| ristocetin A/di-*N*-Ac-Lys-D-Ala-D-Ala | | | 64.3 | |

[a] Data obtained at 280 K and pH 4.5 unless otherwise stated, except those for $\Delta G_{lig}$, which are cited simply to indicate the approximate affinities of the ligands for the antibiotic. [b] Absolute errors uncertain, but relative values reliable to within ±0.5 kJ $mol^{-1}$; see the text for details. [c] Williams, D. H.; Cox, J. P. L.; Doig, A. J.; Gardner, M.; Gerhard, U.; Kaye, P. T.; Lal, A. R.; Nicholls, I. A.; Salter, C. J.; Mitchell, R. C. *J. Am. Chem. Soc.* **1991**, *113*, 7020. [d] Searle, M. S.; Sharman, G. J.; Groves, P.; Benhamu, B.; Beauregard. D. A.; Westwell, M. S.; Dancer, R. J.; Maguire, A. J.; Try, A. C.; Williams, D. H. *J. Chem. Soc., Perkin Trans. 1* **1996**, 2781. [e] Musette, S. Unpublished data.

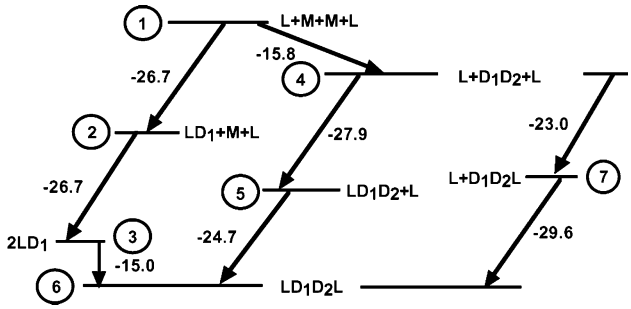


***Figure 5.*** Thermodynamic cycle for the formation of the ligand-bound dimer of ristocetin A (where the ligand is di-*N*-Ac-Lys-D-Ala-D-Ala). Free energy (kJ $mol^{-1}$) is plotted vertically. The numerical values indicate the differences in free energy between connected levels in the directions shown by the arrows.

data for di-*N*-Ac-Lys-D-Ala-D-Ala,[17] the binding of all four ligands appears to be negatively cooperative with respect to dimerization when the criterion for negative cooperativity is the observed relative abundances of monomeric vs dimeric species. The relevant values of $K_{dim}$ and $\Delta G_{dim}$ obtained in the present work are summarized in Table 1, where the free energies of ligand binding (available from previous work) are also given.

The data tell us that, for all four of the above ligands, $LD_1D_2L$ is thermodynamically less stable relative to $2LD_1$ than is $D_1D_2$ relative to 2M. In the case of di-*N*-Ac-Lys-D-Ala-D-Ala as the ligand, the free energy difference is 0.8 ± 0.5 kJ $mol^{-1}$ (Figure 5, level 3 → level 6 vs level 1 → level 4). In the case of Ac-Gly and Ac-Gly-Gly as the ligands, it is 1.3 ± 0.5 and 1.8 ± 0.5 kJ $mol^{-1}$ (Table 1). These energy differences are small, but they are reliable. The reliability arises because differences in free energy changes, for dimerization in the absence or presence of ligand, and for binding of ligand to the $D_2$ vs $D_1$ sites, are determined by direct observation of population differences in the proton NMR spectra. From the Boltzmann equation, a population ratio of 10 corresponds to a difference in free energy of 5.7 kJ $mol^{-1}$ at room temperature. Since population ratios not far from unity can be reliably measured to within a factor of 0.1, the relative energy levels are determined within ±0.5 kJ $mol^{-1}$ in the above instances.

However, the sharpening of the rhamnose 6-methyl resonances in all the sites upon ligand binding (Figure 4) establishes, as in the case of di-*N*-Ac-Lys-D-Ala-D-Ala as ligand,[17] that the

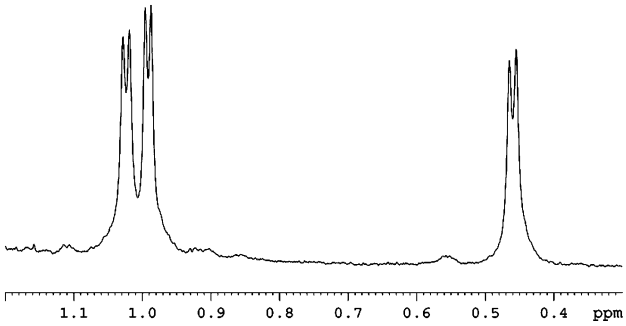


***Figure 6.*** The 0.3−1.2 ppm region of the 700 MHz NMR spectrum of 0.05 mM ristocetin A (at which concentration only monomeric antibiotic is present) in the presence of an excess of di-*N*-Ac-Lys-D-Ala-D-Ala. The intense signals are due to binding in the high-affinity site of M: rhamnose 6-methyl group (0.99 ppm), and the central (1.03 ppm) and C-terminal (0.46 ppm) D-Ala methyl groups of the ligand.

barrier to monomer/dimer exchange is always increased upon ligand binding. These increased barriers have been measured (using the criterion of coalescence) for all four ligands mentioned above (Table 1). It is clear in these cases that the barrier to dimer dissociation increases gradually as the ligands make more interactions with the antibiotic (and bind with increasing affinities, Table 1). This can be seen not only from the measured barriers ($\Delta G^{\ddagger}$, Table 1), but also from the increased sharpness of the methyl resonance signals (Figure 4) in the series (a) → (b) → (c) → (d). Indeed, the doublet nature of the methyl resonances is increasingly evident on passing from (c) to (d). Although the absolute errors in the $\Delta G^{\ddagger}$ values are uncertain, their relative values are reliable to within $\pm 0.5$ kJ mol$^{-1}$. This is because the *differences* in coalescence temperatures for the $D_1$, $D_2$, and M resonances, in the absence and the presence of the various ligands, are reliable and reproducible.

In summary, the above increases in barriers provide a criterion for positive cooperativity between ligand binding and dimerization. Yet the changes in dimer populations ($\Delta G_{\mathrm{dim}}$ values of Table 1) appear to be inconsistent with this conclusion. The dilemma is solved by an analysis (with representation of ligands by L) of the various binding processes in a thermodynamic cycle (Figure 5). The data used in this cycle are those of Cho et al. for the binding of di-*N*-acetyl-Lys-D-Ala-D-Ala to ristocetin A,[17] and are briefly discussed below.

**(ii) Analysis of a Thermodynamic Cycle for Binding.** From the published work,[17] the energy of binding of two di-*N*-Ac-Lys-D-Ala-D-Ala molecules to $D_1D_2$ is −52.6 kJ mol$^{-1}$ (sum of −27.9 and −24.7 kJ mol$^{-1}$, Figure 5, level 4 → level 6). From UV binding studies (carried out at very low concentrations), the energy of binding of the ristocetin A monomer to di-*N*-Ac-Lys-D-Ala-D-Ala is −26.7 kJ mol$^{-1}$ (Figure 5, level 1 → level 2). Therefore, the free energy difference between levels 1 and 3 is $-26.7 \times 2$, i.e., −53.4 kJ mol$^{-1}$. We now show, by NMR spectroscopy, that this binding energy corresponds to binding of the ligand only to the best available binding site of M (a $D_1$-type site; see earlier). Thus, we obtained the proton NMR spectrum of 0.05 mM ristocetin A (at which concentration only the antibiotic monomer is present) in the presence of an excess of di-*N*-Ac-Lys-D-Ala-D-Ala. The 0.3−1.2 ppm region of this spectrum (Figure 6) contains signals due to the rhamnose 6-methyl (0.99 ppm), and due to the central (1.03 ppm) and C-terminal (0.46 ppm) D-Ala methyl groups of the ligand bound to the higher affinity ($D_1$-type) site of the monomer. These assignments were established by saturation transfer experiments, in which the D-Ala methyl signals of the excess of di-*N*-Ac-Lys-D-Ala-D-Ala were irradiated. The small and broad signal at 0.55 ppm is not removed upon irradiation of the 0.46 ppm signal, and therefore, these two signals are not in exchange on the NMR time scale. Thus, the peak at 0.55 ppm does not arise from ligand binding to a $D_2$-type site of M. The well-defined nature of the signals at 1.03, 0.99, and 0.46 ppm, lacking signs of any shoulders, precludes a significant population of a $D_2$-type site of the monomer. Therefore, when $LD_1D_2L$ is formed from two molecules of ligand-bound monomer (Figure 5, level 3 → level 6), it must be formed from $2LD_1$.

The free energy of dimerization of ligand-bound monomer ($2LD_1 \rightarrow LD_1D_2L$) is known to be 0.8 kJ mol$^{-1}$ less favorable than that of ligand-free monomer, and has a value of −15.0 kJ mol$^{-1}$ (Figure 5, level 3 → level 6). Thus, the energy level of $2LD_1$ is available not only from the path 1 → 3 (see above), but also from an analysis involving the path 1 → 4 → 5 → 6 → 3 of Figure 5, and a thermodynamic cycle is thereby closed (Figure 5). We emphasize that the energy levels of $2LD_1$ obtained by the two paths are not independent. This is because the NMR-based binding constants (for ligands to dimeric species) are derived in part[17] from the binding constant of ligand to monomer (based on UV data). However, the completion of the cycle allows a step-by-step analysis of the binding energies.

**(iii) Cost of Occupying a $D_2$ Site vs a $D_1$ Site in the Dimer.** The analysis (Figure 5) points to the reason the population of dimer falls upon ligand binding. $D_1$-type sites bind ligand better than $D_2$-type sites, and occupation of a $D_2$ site by ligand occurs only in $LD_1D_2L$ (where it is mandatory, Figure 3). Therefore, there is discrimination against the association $2LD_1 \rightarrow LD_1D_2L$, relative to $2M \rightarrow D_1D_2$. But this discrimination corresponds to a free energy difference of only 0.8 kJ mol$^{-1}$. Yet the cost of occupying a $D_2$ site relative to a $D_1$ site in the dimer is much larger (4.9 kJ mol$^{-1}$, Figure 5). This is true whether these sites are filled before (level 4 → level 7 vs level 4 → level 5) or after (level 7 → level 6 vs level 5 → level 6) occupation of the other ligand binding site in the dimer. So, the key question is why the discrimination against dimerization, caused by ligand binding, is remarkably small (0.8 kJ mol$^{-1}$), despite the forced occupation of a $D_2$ site in the dimer, relative to binding to a $D_1$ site, being much more costly (4.9 kJ mol$^{-1}$, Figure 5). We conclude in the following sections that it is small due to the benefits of positive cooperativity between dimerization and ligand binding.

**(iv) Effect of Positively Cooperative Binding on the Main Ligand−Receptor Hydrogen Bond Strength.** First, we present evidence, based upon proton NMR chemical shifts, for *local* positively cooperative effects in the binding of ligand to monomer vs dimer. When the size of a hydrogen bond network is increased without the introduction of distortions [(a) → (b) in Figure 1], positively cooperative binding can result in the mutual strengthening (i.e., shortening) of hydrogen bonds. The positively cooperative binding within $LD_1D_2L$ should therefore cause a downfield shift of an amide NH[22,23] within the cooperative framework if an amide NH probe with suitable sensitivity is available. Such a probe is provided by the amide

(22) Wagner, G.; Pardi, A.; Wüthrich, K. *J. Am. Chem. Soc.* **1983**, *105*, 5948−5949.
(23) Wishart, D. S.; Sykes, B. D.; Richards, F. M. *J. Mol. Biol.* **1991**, *222*, 311−333.

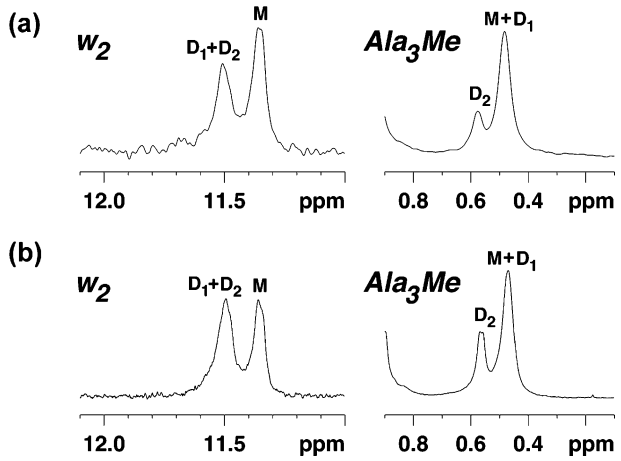


***Figure 7.*** Regions of the proton NMR spectrum (9:1 $H_2O/D_2O$, pH 4.5, and 300 K) of the ristocetin A/di-*N*-Ac-Lys-D-Ala-D-Ala complex at a concentrations of (a) 2 mM and (b) 6 mM.

NH resonance of residue 2 (Figure 2, $w_2$) of ristocetin A, which undergoes a downfield shift in excess of 3 ppm on binding di-*N*-Ac-Lys-D-Ala-D-Ala.[24]

Proton NMR spectra of solutions containing 2 and 6 mM ristocetin A bound to a variety of ligands were obtained. There is clearly the potential to observe three peaks representing each antibiotic proton in the bound state, i.e., two peaks due to binding in the $D_1$ and $D_2$ sites, and one peak due to binding in the M site. When the antibiotic is fully bound to ligand, the two peaks due to each half of the dimer should be equally populated. Since the dimerization constant of the antibiotic bound to di-*N*-Ac-Lys-D-Ala-D-Ala is known (see earlier), we can calculate that in the solution where the antibiotic is 6 mM, the three peaks should be of similar intensity. However, at 2 mM the peak due to monomer should have ca. 2× the intensity of each of the two peaks due to the dimer. The differences in the spectra at the two concentrations should therefore allow the peaks due to monomer and dimer to be distinguished from each other.

The ligands used in these studies included three of the four already studied in this paper (Ac-Gly-Gly, Ac-Gly-Gly-Gly, and di-*N*-Ac-Lys-D-Ala-D-Ala), supplemented by Ac-D-Ala, Ac-D-Ala-Gly, Ac-Gly-D-Ala, and Ac-D-Ala-D-Ala. In each case, the ligand concentration used was such that >90% of the antibiotic would be bound at the end of the titration. The resonance to be followed throughout the titrations, $w_2$, is moved so far downfield (to chemical shift values >10 ppm) that it can be observed in a region of the spectrum unhindered by other resonances.

Figure 7 shows the regions of the spectra containing the $w_2$ resonances (11−12 ppm region), at ristocetin A concentrations of 2 and 6 mM, for the final points of the titrations of di-*N*-Ac-Lys-D-Ala-D-Ala into the two antibiotic solutions, i.e., when all of the antibiotic is bound by ligand. Also shown are the regions of the same spectra containing the resonances due to the C-terminal alanine methyl group ($Ala_3Me$ peaks, 0.2−0.8 ppm) of the bound ligand. In the 6 mM spectrum, there are two peaks due to $w_2$, with chemical shifts of 11.51 and 11.35 ppm. In the spectrum with 2 mM ristocetin A, the same two peaks can be seen except that the peak at 11.35 ppm is now more intense than the other peak. This peak at 11.35 ppm must therefore be due to ristocetin A monomer bound to ligand, as the relative monomer population is greater at this concentration, a fact which is confirmed by comparison with the intensities of the $Ala_3Me$ peaks. Using the relative intensities of the $w_2$ peaks and the $Ala_3Me$ peaks, it was determined that the peak at 11.51 ppm contains the resonances for $w_2$ in both halves of the dimer.

***Table 2.*** Limiting Chemical Shifts of $w_2$ of Monomeric and Dimeric Ristocetin When Fully Bound by a Variety of Truncated Bacterial Cell Wall Precursor Analogues at pH 4.5 and 300 K

| ligand | $\delta w_2$ (monomer) | $\delta w_2$ (dimer)[a] | ligand | $\delta w_2$ (monomer) | $\delta w_2$ (dimer)[a] |
|---|---|---|---|---|---|
| $Ac_2$-Lys-D-Ala-D-Ala | 11.35 | 11.51 | Ac-D-Ala | 10.93 | 11.02 |
| | | | Ac-Gly- | 10.32 | 10.96/10.92 |
| Ac-D-Ala-D-Ala | 11.40 | 11.50 | Gly-Gly | | |
| Ac-D-Ala-Gly | 11.12 | 11.26 | Ac-Gly-Gly | 10.34 | 10.91/10.60 |
| Ac-Gly-D-Ala | 11.07 | 11.12 | | | |

[a] The values for $w_2$ in each half of the dimer were only resolved when the ligand bound was Ac-Gly-Gly-Gly and Ac-Gly-Gly. It is possible that the values with these two ligands are not quite limiting due to the low binding constants of these ligands to ristocetin A. All values are in parts per million relative to the peak for internal TSP ($\delta$ 0 ppm).

Similar results were obtained for the other ligands, and Table 2 summarizes the limiting chemical shifts of $w_2$ for dimeric and monomeric ristocetin A determined from these titrations. The resonances due to $w_2$ in the $D_1$ and $D_2$ sites are coincident in all cases except for the binding of Ac-Gly-Gly and Ac-Gly-Gly-Gly. These are the ligands of lowest affinity for the antibiotic, and it is possible that the noncoincidence of the $w_2$ resonances in these cases arises due to the incomplete saturation of the lower affinity $D_2$ site.

The data in Table 2 show that (i) increased limiting chemical shift values of $w_2$ for the binding of each ligand *correlate* with increased overall binding constants (e.g., as measured by UV spectroscopy) of the ligands to ristocetin A and (ii) the $w_2$ peak due to binding to the $D_1$ and $D_2$ sites of the dimer occurs downfield of the $w_2$ peak due to binding to the monomer (a $D_1$ type site). Points i and ii might initially appear inconsistent, since if there were a direct *causal* relationship between the extent of the downfield chemical shift of $w_2$ and the ligand binding constant, then on the basis of Figure 5 the chemical shifts in the three sites would be $D_1 > M > D_2$. But the order is typically $D_1 \approx D_2 > M$, so it must be concluded that the *correlation* observed under point i does not reflect a causal relationship. The extent of the chemical shift change of a resonance upon complex formation (induced by the new environment experienced in the complex) will be larger the more closely the monitored proton approaches that new environmental influence. Thus, the chemical shift change will be larger the deeper the constraining interaction lies in its local enthalpy well (which has the consequence of shortening the noncovalent bond length).[25,26] Thus, $w_2$ is found at lower chemical shift the more deeply the NH···O═C interaction lies inside its local well. It is the positively cooperative binding of the local hydrogen bond network that limits the local motions, and so improves the bonding of this interaction. *Within* either of the chemical shift columns of Table 2, for binding to monomer or dimer, the trend of increasing chemical shifts of $w_2$ with increasing affinity of

(24) Searle, M. S.; Sharman, G. J.; Groves, P.; Benhamu, B.; Beauregard, D. A.; Westwell, M. S.; Dancer, R. J.; Maguire, A. J.; Try, A. C.; Williams, D. H. *J. Chem. Soc., Perkin Trans. 1* **1996**, 2781−2786.

(25) O'Brien, S. W.; Shiozawa, H.; Zerella, R.; O'Brien, D. P.; Williams, D. H. *Org. Biomol. Chem.* **2003**, *1*, 472−477.

(26) Williams, D. H.; Bardsley, B.; O'Brien, D. P. *J. Chem. Soc., Perkin Trans. 2* **2000**, 1682−1684.

ligand largely reflects the manner in which the hydrogen bond to $w_2$ is cooperatively enhanced. The increasing numbers of adjacent and relatively strain-free interactions that the ligand makes with the antibiotic enhance this hydrogen bond strength. The larger chemical shifts found for dimers in comparison to monomers in Table 2 (for any given ligand), reflect the cooperative enhancement of the strength of the hydrogen bond in ligand-bound dimers over ligand-bound monomers.

**(v) Free Energy Benefits of the Positively Cooperative Binding.** We now present evidence for *global* positively cooperative effects in the common sets of interactions involved in the binding of ligand to dimer. This evidence is derived from the thermodynamic data. A meaningful test for cooperativity requires that the interactions when made separately or simultaneously must be *the same in type and number*. Since the following three processes all involve binding ligand (here di-*N*-Ac-Lys-D-Ala-D-Ala) to a $D_1$-type site (see earlier), this condition is fulfilled in these instances [binding energies from Figure 5 (kJ $mol^{-1}$) are given in parentheses]:

$$L + M \rightarrow LD_1\ (-26.7)$$

$$L + D_1D_2 \rightarrow LD_1D_2\ (-27.9)$$

$$L + D_1D_2L \rightarrow LD_1D_2L\ (-29.6)$$

Thus, the binding of di-*N*-Ac-Lys-D-Ala-D-Ala to the $D_1$-type site is positively cooperative by 1.2 kJ $mol^{-1}$ in binding to dimer over binding to monomer. It is positively cooperative by 2.9 kJ $mol^{-1}$ in binding to dimer in which the $D_2$ site is already occupied by ligand over binding to monomer. Analogous to the behavior typically observed in the folding of proteins, the making of the specified set of noncovalent bonds occurs with greater affinity where the binding occurs to the larger assembly.

The $D_2$-type ligand site is not significantly occupied in the monomer (Figure 6). Nevertheless, data with regard to cooperative binding to this site are available (Figure 5):

$$L + D_1D_2 \rightarrow D_1D_2L\ (-23.0)$$

$$L + LD_1D_2 \rightarrow LD_1D_2L\ (-24.7)$$

Thus, ligand binding to the $D_2$ site of the dimer is positively cooperative since it occurs with higher affinity when the $D_1$ site of the dimer is already filled. Once more, the ligand binds to the larger assembly with greater affinity.

**(vi) Effects of Positively Cooperative Binding on the Population of Ligand-Bound Dimer and the Barrier to Its Dissociation.** The formation of $LD_1D_2L$ necessitates the occupation of a $D_2$ site that is less favorable than a $D_1$ site by 4.9 kJ $mol^{-1}$ (section iii). Nevertheless, full ligand binding of the dimer opposes dimerization by only 0.8 kJ $mol^{-1}$ (Figure 5). The difference (4.1 kJ $mol^{-1}$) is due to the benefit of the positive cooperativity in $LD_1D_2L$, arising from mutual reinforcement of noncovalent interactions among the three interfaces shown in Figure 3a.

If the center (dimer) interface of the three is broken, then, by definition, there is no cooperativity in the product $LD_1 + D_2L$. As the dissociation of the ligand-bound dimer proceeds to its transition state ($LD_1D_2L \rightarrow LD_1\cdots D_2L$, Figure 3b), a free energy cost of occupying the $D_2$ site (as opposed to a $D_1$ site) with ligand remains. Therefore, the benefit of positively cooperative binding (−4.1 kJ $mol^{-1}$) that is present in $LD_1D_2L$ should be largely lost in the transition state ($LD_1\cdots D_2L$) since the center interface of the three is extensively broken. That is, the barrier to $LD_1D_2L \rightarrow LD_1 + D_2L$ should, relative to the barrier to $D_1D_2 \rightarrow D_1 + D_2$, be raised due to the loss of positive cooperativity during the dissociation process. The barriers to dissociation of the ristocetin A dimer both in the presence and in the absence of the ligands Ac-Gly, Ac-Gly-Gly, Ac-Gly-Gly-Gly, and di-*N*-Ac-Lys-D-Ala-D-Ala have been determined (Table 1). The prediction is confirmed. It is the differences in the barriers in the presence and absence of ligands, rather than the absolute values of the barriers, that are important. As noted previously, the raised barriers are evidenced by sharper resonances (i.e., slower exchange) for the rhamnose methyl resonances when the $LD_1D_2L \leftrightarrow LD_1 + D_2L$ exchange occurs, in comparison to when the $D_1D_2 \leftrightarrow D_1 + D_2$ exchange occurs (see Cho et al.[17] and Figure 4). As the ligand size (and affinity; see Table 1) is increased in the series Ac-Gly → Ac-Gly-Gly → Ac-Gly-Gly-Gly → di-*N*-Ac-Lys-D-Ala-D-Ala, the barrier to dimer dissociation increases from 1 to 2.1, to 3.1, and finally to 3.8 kJ $mol^{-1}$. This last value is, within experimental error, in agreement with the anticipated increase due to the loss of positive cooperativity (4.1 kJ $mol^{-1}$) in the $LD_1\cdots D_2L$ transition state. The relevant free energy changes are summarized in Figure 8.

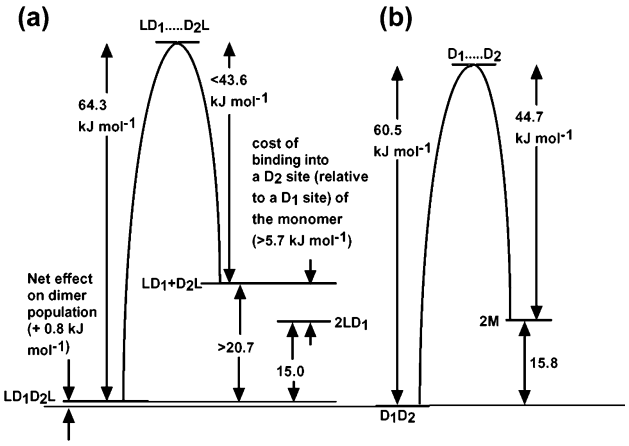


***Figure 8.*** Comparison of the free energy profiles accounting for the relative populations and rates of exchange of ristocetin A dimers in (a) the presence and (b) the absence of ligand. To emphasize the benefits due to positive cooperativity, and costs of occupancy of a $D_2$ site, the a and b portions of the figure are referenced to $2LD_1$ and 2M at the same free energy level. In constructing part a of this figure, we have utilized the fact that the free energy of $D_2L$ must be at least 5.7 kJ $mol^{-1}$ greater than that of $D_1L$ since the former species must have a population which is <10% of the latter (see Figure 6).

**(vii) Wider Implications of the Work for Common Sets of Interactions.** Where ligand binding is not cooperative, a protein receptor structure remains unchanged upon ligand binding (**D** and **C**, Figure 9a). But where it is positively cooperative, the receptor structure tightens (**E** vs **C**, Figure 9a). The physical basis for the structural changes is that positively cooperative binding of the ligand strengthens the hydrogen bonding within the receptor (section iv). This effect should be analogous to the way in which bonding is improved in a solid or liquid upon cooling it. Thus, at a receptor interface that is tightened by the positively cooperative binding of ligand, the amide hydrogen bonds of the internal interface will occupy lower

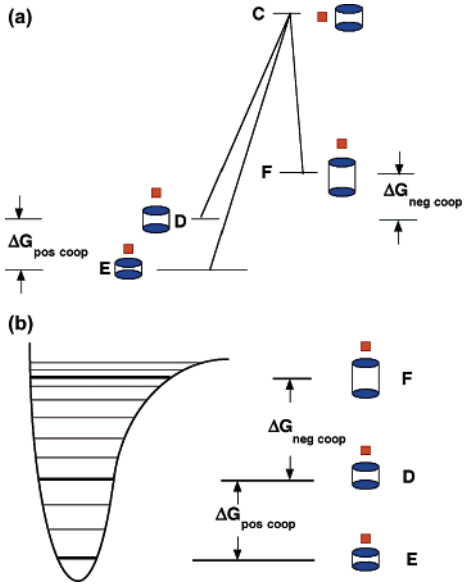


***Figure 9.*** (a) Relative free energies (plotted vertically) of a ligand/receptor system (red square = ligand, blue ellipses = receptor) formed without cooperativity (**D**), with positive cooperativity (**E**), and with negative cooperativity (**F**). (b) Schematic illustration of the relative vibrational levels occupied by an amide−amide hydrogen bond where the hydrogen bond strength and ligand binding are not coupled (**D**), are positively coupled (**E**), and are negatively coupled (**F**).

vibrational levels within their local wells (**E** vs **D**, Figure 9b). *There is a cost in entropy due to this change, but a net benefit in free energy for the formation of the more ordered system because the benefit in enthalpy (*$\Delta H$*, from lying more deeply in the well) outweighs the adverse* $T\Delta S$ *term.* $\Delta G_{\text{pos coop}}$ is obtained by integrating over all the noncovalent interactions that are enhanced in this way. It is for this reason that positively cooperative binding raises the barriers to breaking interfaces (see the preceding section), and reduces the rates of amide H/D exchange.[11] Conversely, at a receptor interface that is loosened by the negatively cooperative binding of ligand, the amide hydrogen bonds of the internal interface should occupy higher vibrational levels within their local wells (**F** vs **D**, Figure 9b). It is for this reason that negatively cooperative binding increases the rates of amide H/D exchange.[11,27]

## Conclusions

The population of an asymmetric dimeric receptor falls upon ligand binding because the $D_2$ ligand binding site in $LD_1D_2L$ has some noncovalent interactions that are unique to this site and less favorable than those occurring in the comparable region of a $D_1$ site. However, the interactions that are common to both the $D_1$ and $D_2$ sites, and those present at the dimer interface (Figure 2), are, by several criteria, mutually reinforcing (i.e., formed with positive cooperativity).

A structural model leads to the conclusion that such positively cooperative binding will reduce the dynamic behavior of the receptor system. A raised barrier to $LD_1D_2L$ dissociation, relative to $D_1D_2$ dissociation, gives evidence for such a reduction in dynamic behavior. It is analogous to the reduced dynamic behavior of proteins upon positively cooperativity binding of ligands, reaction substrates or products, or transition states.[11] Binding of the small molecule is promoted where the receptor protein shows some or all of the following properties: (i) reduced NH to ND exchange,[11,28,29] (ii) a raised melting temperature ($T_m$),[30] (iii) improved internal bonding and reduced dynamic behavior (more negative values of $\Delta H$ and $\Delta S$ for ligand binding[11,31]), and (iv) greater resistance to enzymic digestion and possibly also promotion of the stability of oligomeric forms of the protein.[30] Negatively cooperative binding promotes converse effects.[10,11,32]

The ristocetin A dimer system has proved very useful in establishing general principles since it provides an analogue of a protein receptor. In contrast to a protein receptor, the increased barrier to breaking an internal interface, following ligand binding, can be directly measured.

**Acknowledgment.** We thank BBSRC (N.L.D) and EPSRC (R.Z. and B.B.) for financial support.

**Supporting Information Available:** Experimental details (PDF). This material is available free of charge via the Internet at http://pubs.acs.org.

JA039409P

(27) Englander, S. W.; Englander, J. J.; McKinnie, R. E.; Ackers, G. K.; Turner, G. J.; Westrick, J. A.; Gill, S. J. *Science* **1992**, *256*, 1684−1687.
(28) Wang, F.; Miles, R. W.; Kicsa, G.; Nieves, E.; Schramm, V. l.; Angeletti, R. H. *Protein Sci.* **2000**, *9*, 1660−1668.
(29) Wang, F.; Shi, W.; Nieves, E.; Angeletti, R. H.; Schramm, V. L.; Grubmeyer, C. *Biochemistry* **2001**, *40*, 8043−8054.
(30) Laitinen, O. H.; Marttila, A. T.; Kari, J.; Airenne, K. J.; Kulik, T.; Livnah, O.; Bayer, E. A.; Wilchek, M.; Kulomaa, M. S. *J. Biol. Chem.* **2001**, *276*, 8219−8224.
(31) Weber, P. C.; Wendoloski, J. J.; Pantoliano, M. W.; Salemme, F. R. *J. Am. Chem. Soc.* **1992**, *114*, 3197−3200.
(32) Flatmark, T.; Almas, B.; Knappskog, P. M.; Berge, S. V.; Svebak, R. M.; Chehin, R.; Muga, A.; Martinez, A. *Eur. J. Biochem.* **1999**, *262*, 840−849.